# Anomalous Scaling for Thick Electrodeposited Films

M. C. Lafouresse,[1] P. J. Heard,[2] and W. Schwarzacher[1]

[1]*H. H. Wills Physics Laboratory, Tyndall Avenue, Bristol BS8 1TL United Kingdom*

[2]*Interface Analysis Centre, 121 St. Michael's Hill, Bristol BS2 8BS United Kingdom*

(Received 16 January 2007; published 4 June 2007)

Anomalous surface roughness scaling, where both the local and the large-scale roughness show a power-law dependence on the film thickness, has been widely observed. Here we show that the value of the local roughness exponent in the early stages of Cu electrodeposition depends on the deposition potential. However, initial anomalous scaling can lead to two qualitatively different types of behavior for large film thickness ($t \geq 4$ $\mu$m). For Cu films electrodeposited with forced convection at high potential and current density, the anomalous scaling is transient: the local roughness saturates for the thickest films studied. When Cu films are electrodeposited at similar potential and current density but with reduced convection, no saturation of the local roughness is observed. Instead the film forms overhangs such that the surface height becomes a multivalued function of the lateral position.

DOI: 10.1103/PhysRevLett.98.236101 PACS numbers: 68.55.Jk, 81.15.Pq

Kinetic roughening occurs in a wide range of systems where material is added to or removed from a surface far from equilibrium. When both the local and the large-scale roughness show a power-law dependence on the film thickness, the system exhibits "anomalous scaling" [1–4]. Many experimental examples of anomalous surface roughness scaling have been observed, including evaporated single-element metal films [5], metal/metal multilayer films [6], and evaporated polymer films [7]. However, previous experimental studies for evaporated and electrodeposited films [8] were unable to show how the anomalous scaling develops in the thick film limit [9,10]. In this Letter we study films up to tens of $\mu$m thick and demonstrate that within the same experimental system anomalous scaling can either be transient or continue until the film forms overhangs, depending on the deposition conditions.

We study Cu films that show anomalous scaling [11] and use focused ion beam (FIB) imaging to measure the surface width of thick films too rough to quantify with conventional atomic force microscopy (AFM). The films are electrodeposited from organic additive-free acid sulphate electrolytes. Apart from its technical relevance, electrodeposition is of especial interest for thin film growth studies because, unlike sputtering or molecular beam epitaxy, transport of material to the surface is diffusive rather than ballistic, and it is possible to control the thermodynamic driving force for film growth by changing the substrate potential.

For the first time in a kinetic roughening study, we control the bulk mass transport using a rotating disc electrode (RDE). This allows us to vary the deposition potential $E$ and the ratio of the current density $j$ to its diffusion-limited value $j_L$ separately. These parameters are crucial because $E$ controls the thermodynamic driving force and can influence local kinetic parameters such as the surface diffusion coefficient while $j/j_L$ indicates how likely the growth is to be controlled by bulk mass transport. We show that in the early stages of growth the local roughness exponent $\beta_{\mathrm{loc}}$ is, to a good approximation, a single-valued function of $E$, but that for fixed $E$ different values of $j/j_L$ give a different roughness evolution in the later stages of growth.

The roughness of a growing film may be characterized by the thickness- and scale-dependent surface width $w(l, t)$, defined as

$$w(l, t) = \sqrt{\langle [h(t) - \langle h(t) \rangle]^2 \rangle}, \tag{1}$$

where $h$ is the height of the surface, $l$ is the length-scale over which $w$ is measured and $t$ the film thickness, or for films grown at constant rate, the deposition time. For many real and model systems $w(l, t)$ has been found to follow power laws of the form:

$$\begin{aligned} w(l, t) &\propto l^H t^{\beta_{\mathrm{loc}}} \quad \text{for } l \ll l_c \\ w(l, t) &\propto t^{\beta + \beta_{\mathrm{loc}}} \quad \text{for } l \gg l_c, \end{aligned} \tag{2}$$

where $H$ is the so-called Hurst exponent, $l_c$ is a crossover length, and $\beta$ is the growth exponent [1]. If the local exponent $\beta_{\mathrm{loc}}$ is nonzero, the system is said to exhibit anomalous scaling; otherwise normal (Family-Vicsek) scaling applies [1,12]. The crossover length scales as $l_c \propto t^{1/z}$, and to ensure consistency, $z = H/\beta$. For a film made up of smooth mounds, $l_c$ is a measure of the average mound size and $w_{\mathrm{sat}}$ [$= w(l, t)$ for $l \gg l_c$] is the corresponding mound height. For such a film $H \sim 1$, and it follows that the mound aspect ratio $w_{\mathrm{sat}}/l_c \propto t^{\beta_{\mathrm{loc}}}$ [13]. A nonzero $\beta_{\mathrm{loc}}$ therefore means that the aspect ratio increases with increasing film thickness; i.e., the surface features become sharper.

Cu thin films were electrodeposited from an organic additive-free $0.03M$–$0.6M$ $CuSO_4$/$1.2M$ $H_2SO_4$/$0.25$ m$M$

 

KCl electrolyte. The $Cl^-$ is an important constituent of this electrolyte as $Cl^-$ adsorbs strongly on Cu and affects the surface structure [14]. As in previous studies, films of different thickness were deposited galvanostatically (i.e., at constant current). The deposition potential was measured with respect to a mercury sulphate reference electrode (MSE).

Convection was controlled using a RDE. Varying the angular velocity $\omega$ of the RDE varies the effective thickness $\delta$ of the diffusion layer. Assuming a linear concentration profile and Tafel kinetics,

$$j/j_L = [1 + D\exp(-\alpha n e\eta/kT)/j_0\delta]^{-1}, \qquad (3)$$

where $D$ is the bulk diffusion constant, $j_0$, $\alpha$, and $n$ are constants for a given electrochemical reaction, and $\eta$ is the overpotential [15]. Since $\eta = |E - E_0|$, where $E_0$ is the equilibrium potential of the metal ion reaction at the working electrode, it is clear that $E$ and $j/j_L$ may be varied independently by controlling $\delta$.

Substrates were prepared by sputtering Au(100 nm)/Cr(50 nm) on 0.5 cm diameter glass disks that could easily be fitted to the RDE. Following growth, the film surface was imaged by contact mode AFM with a resolution of $256 \times 256$ pixels. Cross sections of the thickest films were obtained and imaged using a FIB, as AFM data are not reliable when the roughness becomes too high. Smoothing was applied to the data to remove short-range noise. $w(l, t)$ data obtained from AFM and FIB measurements of the same films are in excellent agreement [15]. Values of $w_{\mathrm{sat}}$, $l_c$ and $H$ were extracted from the $w(l, t)$ data by fitting with the function $w(l, t) = w_{\mathrm{sat}}(t)(1 - \exp\{-[l/l_c(t)]^H\})$ [16].

To investigate the dependence of $\beta_{\mathrm{loc}}$ on $E$ for constant $j/j_L$, we compared series of films (i) deposited from an unstirred electrolyte containing $0.6M$ $CuSO_4$ at $E = -0.44 \pm 0.01$ V and $j = 6$ mA cm$^{-2}$, and (ii) deposited from an electrolyte containing $0.3M$ $CuSO_4$ at $j = 45$ mA cm$^{-2}$ and $E = -0.60 \pm 0.01$ V with the RDE rotating at 4000 rpm. For both series of films, $j/j_L$ was $\sim 0.1$ (the error in all quoted values of $j/j_L$ is approximately $\pm 0.03$). Figure 1 shows AFM $w(l, t)$ data from the films, together with sample FIB images. The behavior for $l \ll l_c$ is clearly different for the two series, though both show anomalous scaling. For (i) $\beta_{\mathrm{loc}} = 0.07 \pm 0.03$ and $\beta = 0.21 \pm 0.05$, while for (ii) $\beta_{\mathrm{loc}} = 0.44 \pm 0.04$ and $\beta = 0.29 \pm 0.05$. This experiment demonstrates for the first time the sensitivity of $\beta_{\mathrm{loc}}$ to $E$, without changing $j/j_L$ [17].

Figure 2 shows the variation of $\beta_{\mathrm{loc}}$ with $E$, measured for thicknesses in the range $t = 250$ nm to 4 $\mu$m, and many different electrolyte concentrations, rotation speeds and current densities. Note that all the data points lie on, or close to, a single curve, i.e., to a good approximation $\beta_{\mathrm{loc}}$ is a single-valued function of $E$. For example, for film thickness $t \leq 4$ $\mu$m, and fixed $E = -0.6 \pm 0.02$ V, within error $\beta_{\mathrm{loc}}$ does not vary when $j/j_L$ is varied over the full range $0.1 \leq j/j_L \leq 0.8$.

One reason for $\beta_{\mathrm{loc}}$ to depend on the deposition potential is that the latter strongly affects the mobility of metal adatoms [18,19], and this influences the film microstructure and morphology. For vapor-deposited polycrystalline

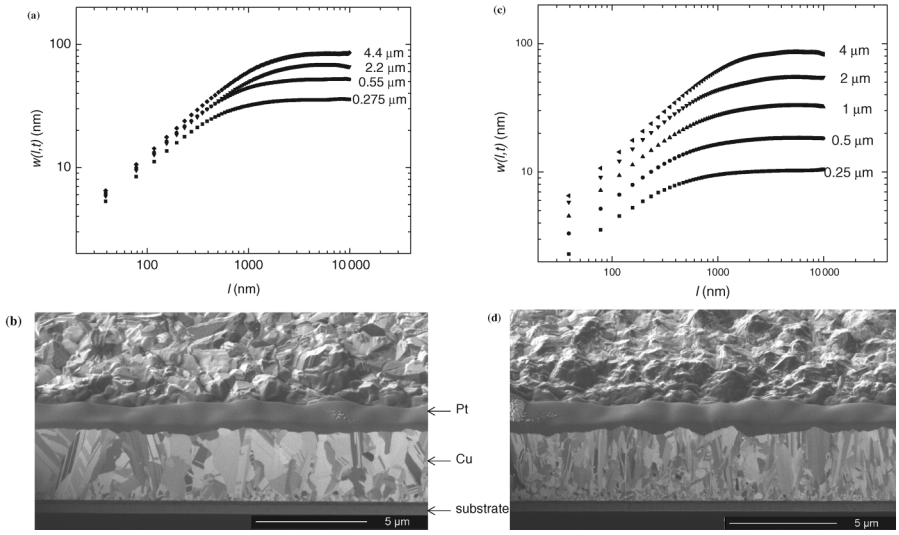


FIG. 1. (a) $w(l, t)$ (rms surface width as a function of length-scale) measured by AFM for a series of films electrodeposited without rotation from a $0.6M$ $CuSO_4/1.2M$ $H_2SO_4/0.25$ m$M$ KCl electrolyte at a current density of 6 mA cm$^{-2}$. $j/j_L \sim 0.1$, $E = -0.44 \pm 0.01$ V. (b) FIB image from a film of total thickness $\sim 4$ $\mu$m deposited for 32 minutes under these conditions. The sample tilt is 45°. The Pt strip is deposited to protect the surface while etching using the FIB. (c) $w(l, t)$ data for a series of films deposited from a $0.3M$ $CuSO_4/1.2M$ $H_2SO_4/0.25$ m$M$ KCl electrolyte at a current density of 45 mA cm$^{-2}$ on a RDE rotating at 4000 rpm. $j/j_L \sim 0.1$, $E = -0.60 \pm 0.01$ V (d) FIB image from a film of total thickness 4 $\mu$m deposited for 4 min under the same conditions. The sample tilt is 45°.

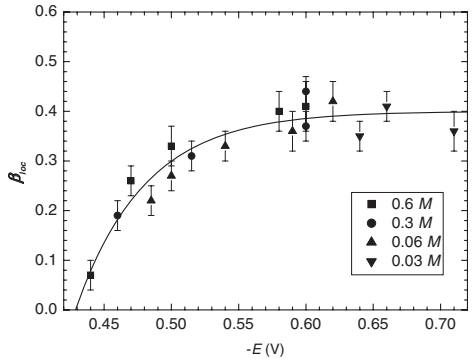


FIG. 2. $\beta_{\mathrm{loc}}$ measured for films in the thickness range $t =$ 250 nm to 4 $\mu$m, grown galvanostatically from different concentration electrolytes (shown on figure) at different rotation speeds plotted as a function of deposition potential $-E$. The solid line is a guide to the eye.

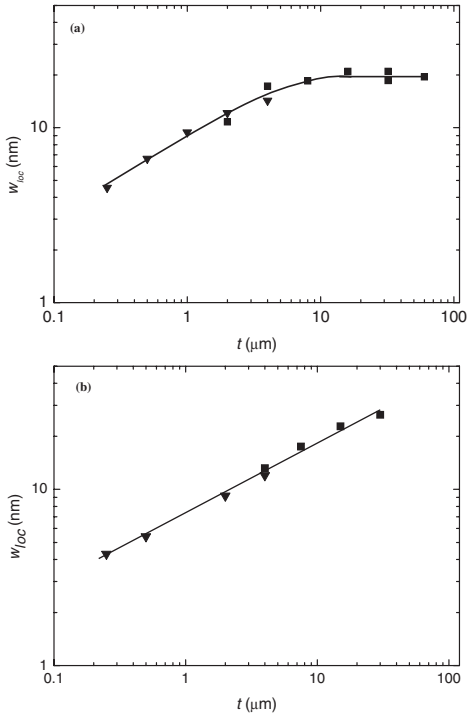


FIG. 3. (a) Local roughness $w_{\mathrm{loc}} = w(x, t)$, where $x = 117$ nm (which is much less than $l_c$ for all thicknesses $t$ considered), measured for a series of films electrodeposited from a 0.3$M$ $CuSO_4$/1.2$M$ $H_2SO_4$/0.25 m$M$ KCl electrolyte at a current density of 45 mA cm$^{-2}$ on a RDE rotating at 4000 rpm. $E = -0.6$ V, $j/j_L \sim 0.1$. Data points (▼) were obtained by AFM, while data points (■) were obtained from FIB images. The solid line is a guide to the eye. (b) As (a) but for a current density of 30 mA cm$^{-2}$ on a RDE rotating at 100 rpm. $E = -0.6$ V, $j/j_L \sim 0.6$.

films, increased surface mobility contributes to the increased lateral grain size observed with increasing substrate temperature [20]. Comparison of FIB images of two films with the same thickness $t \sim 4$ $\mu$m grown at different deposition potentials $E = -0.44$ V [Fig. 1(b)] and $E = -0.60$ V [Fig. 1(d)] reveals that at more positive potentials (where the mobility is expected to be greater), the lateral grain size is indeed greater. Another reason for the morphology to depend on the deposition potential is that defects such as twinning are more likely at higher overpotentials. One might also expect enhanced nucleation of new grains at higher overpotentials [21].

New effects are seen when the film thickness increases beyond the range covered by Fig. 2. Figure 3(a) shows that the anomalous scaling observed for small $t$ when $E = -0.6$ V, $j = 45$ mA cm$^{-2}$ and $\omega = 4000$ rpm [$j/j_L \sim 0.1$: the conditions of Figs. 1(c) and 1(d)] is a transient effect, because for $t > \sim 4\mu$m the local roughness $w_{\mathrm{loc}}$ saturates. Quite similar behavior has been observed very recently for Cu electrodeposition in the absence of $Cl^-$, where the deposition was also carried out far from the diffusion limiting current [22]. The saturation of $w_{\mathrm{loc}}$ is correlated with the microstructure, because x-ray diffraction studies of our films show that it coincides with the establishment of a dominant {110} texture. Electrocrystallization studies of Ag suggest that repeated twinning at high overpotential gives rise to clusters of ⟨110⟩-oriented crystallites with a characteristic morphology that eventually dominate the growth because they contain an extremely high density of active sites and therefore grow especially rapidly [23].

Very different behavior is seen in Fig. 3(b), which shows how the local roughness $w_{\mathrm{loc}}$ varies with thickness for a series of films electrodeposited from the same 0.3$M$ $CuSO_4$/1.2$M$ $H_2SO_4$/0.25 m$M$ KCl electrolyte as the films of Fig. 3(a), but with current density 30 mA cm$^{-2}$, and the RDE rotating at 100 rpm. The deposition potential measured during growth was $-0.60 \pm 0.01$ V relative to MSE. Under these conditions, the local roughness increases according to a power law $w_{\mathrm{loc}} \propto t^{\beta_{\mathrm{loc}}}$ with $\beta_{\mathrm{loc}} = 0.37 \pm 0.04$ over the whole thickness range shown (2 orders of magnitude). There is no evidence of saturation, even though the deposition potential for these films is the same within error as for those of Fig. 3(a) and the current density is actually less. However, the ratio $j/j_L \sim 0.6$ is much higher, so that the system is much closer to being diffusion limited. The continued increase in $w_{\mathrm{loc}}$, despite the establishment of a dominant {110} texture as before, is therefore likely to be due to a diffusional instability, whereby metal ions diffuse preferentially towards protrusions, amplifying any existing roughness [17]. This type of instability is closely related to the Mullins-Sekerka instability [24].

If the local roughness does not saturate, what happens as the film thickness continues to increase? In the case of films grown at $j = 30$ mA cm$^{-2}$ and $\omega = 100$ rpm, overhangs form as shown in Fig. 4(a), the surface height becomes a multivalued function of the lateral position, and $w(l, t)$ no longer has a clear meaning. At even higher potentials spheroidal nodules form [Fig. 4(b)]. A qualita-

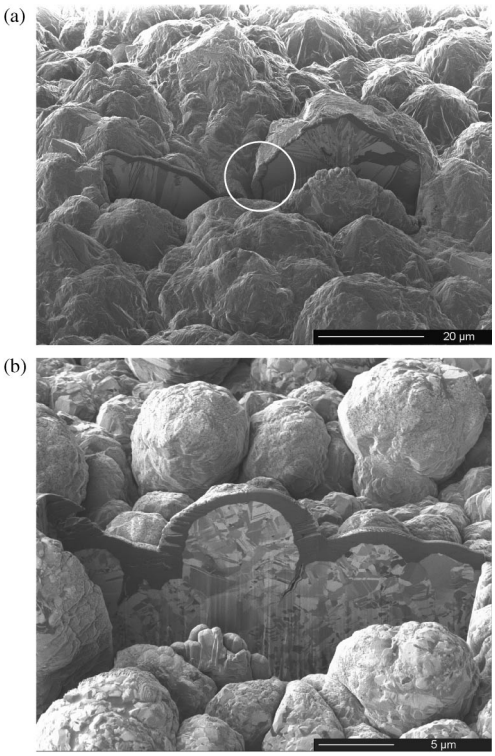


FIG. 4. (a) Typical FIB image from a film of average thickness 60 $\mu$m deposited for 90 minutes from a 0.3$M$ $CuSO_4$/1.2$M$ $H_2SO_4$/0.25 m$M$ KCl electrolyte at a current density of 30 mA cm$^{-2}$ on a RDE rotating at 100 rpm, showing the formation of overhangs (circled). The deposition potential $E = -0.60 \pm 0.01$ V and $j/j_L \sim 0.6$. (b) FIB image of a film of average thickness 11 $\mu$m electrodeposited from an electrolyte containing 0.03$M$ $CuSO_4$ at a current density of 16 mA cm$^{-2}$ on a RDE rotating at 800 rpm. $E = -0.75 \pm 0.01$ V and $j/j_L \sim 0.8$. For both images, the sample tilt is 45°.

tively similar morphology evolution has been seen for Cu electrodeposition in (1 + 1)-dimensional growth [25].

To summarize, we have used controlled convection with a RDE to vary the current density $j$, deposition potential $E$, and the ratio $j/j_L$ independently, for the first time in a kinetic roughening study. We find that for Cu electrodeposited from a $Cl^-$-containing electrolyte the power-law exponent $\beta_{loc}$ describing the evolution of the local roughness $w_{loc}$ with film thickness $t$ is strongly dependent on the deposition potential $E$ during the early stages of growth. During the later stages of growth at high potentials, $w_{loc}$ either saturates or continues increasing until overhangs develop, depending on how close the bulk mass transport is to being diffusion limited. In the former case, the saturation of $w_{loc}$ reflects the development of a dominant crystalline texture, while in the latter case the diffusional instability causes $w_{loc}$ to continue to increase. These results provide insight into how anomalous scaling develops in thicker films, and demonstrate the role of potential and mass transport in controlling the morphology of electrodeposits.

This work is supported by the UK Engineering and Physical Sciences Research Council.

[1] P. Meakin, *Fractals, Scaling and Growth far from Equilibrium* (Cambridge University Press, Cambridge, England, 1998).
[2] M. Schroeder, M. Siegert, D. E. Wolf, J. D. Shore, and M. Plischke, Europhys. Lett. **24**, 563 (1993).
[3] J. M. López, Phys. Rev. Lett. **83**, 4594 (1999).
[4] J. M. López, M. Castro, and R. Gallego, Phys. Rev. Lett. **94**, 166103 (2005).
[5] G. Palasantzas, Phys. Rev. E **56**, 1254 (1997).
[6] J. Santamaria, M. E. Gómez, J. L. Vicent, K. M. Krishnan, and I. K. Schuller, Phys. Rev. Lett. **89**, 190601 (2002).
[7] Y.-P. Zhao, J. B. Fortin, G. Bonvallet, G.-C. Wang, and T.-M. Lu, Phys. Rev. Lett. **85**, 3229 (2000).
[8] M. Saitou, Phys. Rev. B **66**, 073416 (2002).
[9] M. Castro, R. Cuerno, A. Sánchez, and F. Domínguez-Adame, Phys. Rev. E **57**, R2491 (1998).
[10] R. Cuerno and M. Castro, Phys. Rev. Lett. **87**, 236103 (2001).
[11] S. Huo and W. Schwarzacher, Phys. Rev. Lett. **86**, 256 (2001).
[12] F. Family and T. Vicsek, J. Phys. A **18**, L75 (1985).
[13] J. Krug, Physica (Amsterdam) **A263**, 170 (1999).
[14] M. R. Vogt, F. A. Möller, C. M. Schilz, O. M. Magnussen, and R. J. Behm, Surf. Sci. **367**, L33 (1996).
[15] M. C. Lafouresse, P. J. Heard, and W. Schwarzacher (to be published).
[16] S. K. Sinha, E. B. Sirota, S. Garoff, and H. B. Stanley, Phys. Rev. B **38**, 2297 (1988).
[17] W. Schwarzacher, J. Phys. Condens. Matter **16**, R859 (2004).
[18] M. Giesen, G. Beltramo, S. Dieluweit, J. Müller, H. Ibach, and W. Schmickler, Surf. Sci. **595**, 127 (2005).
[19] K. Krug, J. Stettner, and O. M. Magnussen, Phys. Rev. Lett. **96**, 246101 (2006).
[20] C. R. M. Grovenor, H. T. G. Hentzell, and D. A. Smith, Acta Metall. **32**, 773 (1984).
[21] E. Budevski, G. Staikov, and W. J. Lorenz, *Electrochemical Phase Formation and Growth* (VCH, Weinheim, 1996).
[22] A. Osafo-Acquaah, Y. Shapir, and J. Jorne, J. Electrochem. Soc. **153**, C535 (2006).
[23] N. Pangarov and V. Velinov, Electrochim. Acta **13**, 1641 (1968).
[24] W. W. Mullins and R. F. Sekerka, J. Appl. Phys. **35**, 444 (1964).
[25] G. L. M. K. S. Kahanda, X.-Q. Zou, R. Farrell, and P.-Z. Wong, Phys. Rev. Lett. **68**, 3741 (1992).